

Statistical Analysis of Turbulent Premixed Flame Propagation in Droplet-laden Mixtures: A Direct Numerical Simulation Investigation

Daniel H. Wacks, Nilanjan Chakraborty

School of Mechanical and Systems Engineering, Newcastle University
Stephenson Building, Claremont Road, Newcastle upon Tyne, NE1 7RU, UK
daniel.wacks@ncl.ac.uk; nilanjan.chakraborty@ncl.ac.uk

Abstract- A detailed parametric analysis of premixed flame propagation in n-decane droplet-laden mixtures has been carried out under decaying turbulence for different values of overall equivalence ratio (ϕ_{ov}), root-mean-square velocity fluctuation (u'), longitudinal integral length scale (L_{11}) and droplet diameter (a_d) using three-dimensional Direct Numerical Simulations (DNS). Fuel exists both in liquid and gaseous phases in the current analysis where the liquid phase consists of sub-grid droplets which are introduced into the unburned gas, upstream of the premixed flame front. The introduction of droplets into the unburned gas is performed in such a way so as to maintain a constant group number (G) in all two-phase simulations. An initially stoichiometric premixed flame front is then allowed to propagate into the droplet-laden mixtures and the subsequent flame propagation behaviour has been compared with corresponding statistics obtained from the stoichiometric premixed flame simulations. The statistical nature of the flame propagation for small droplets has been found to be comparable to those for the premixed flame simulations, whereas cases with larger droplets exhibit evidence of droplet-induced effects such as reduced gaseous fuel reaction rate and increased flame thickness. Droplets were observed to evaporate both in the unburnt and, especially for droplets of larger diameter, in the burnt regions, enhancing the gaseous fuel mass fraction on both sides of the flame front. It has also been found that, although the overall equivalence ratio far exceeded stoichiometric mixture conditions, the reaction takes place predominantly under fuel-lean conditions.

Keywords: Premixed flame, Direct Numerical Simulation (DNS), Droplet, Reaction rate, Molecular diffusion rate

1. Introduction

The propagation of flames in droplet-laden mixtures is of fundamental importance in a number of engineering applications such as Internal Combustion engines, aero-gas turbines (Aggarwal, 1998) and hazard prediction and control (Bowen, 2011). A number of experimental (Burgoyne and Cohen, 1954, Faeth, 1987, and Lawes and Saat, 2011) and numerical (Miller and Bellan, 1999, Reveillon and Vervisch, 2005, and Wandel et al., 2009) investigations have been carried out revealing the importance of turbulence intensity, droplet diameter, number density and droplet evaporation characteristics on the nature of flame-droplet interaction, both with regard to flame propagation and burning rate. It was also observed that the equivalence ratio of the gaseous mixture following evaporation had an influence on flame propagation under laminar conditions. Despite the wealth of experimental and numerical data on droplet and spray combustion already available, an extensive and systematic parametric analysis of premixed flame propagation in droplet-laden mixtures has not yet been performed. This Direct Numerical Simulation (DNS) investigation aims to provide a first

step towards a deeper understanding of premixed flame propagation in droplet-laden mixtures for different values of overall equivalence ratio, root-mean-square (rms) velocity fluctuation, longitudinal integral length scale and droplet diameter.

Previous numerical studies (Miller and Bellan, 1999, Reveillon and Vervisch, 2005, and Wandel et al., 2009) employing 3D DNS of turbulent combustion of droplet-laden mixtures have treated droplets as sub-grid particles, which were tracked in the Lagrangian sense, whilst the gaseous phase was dealt with in typical Eulerian fashion. Contributions to mass, momentum and energy from the evaporation of droplets were introduced via appropriate source terms into the Eulerian phase. The present analysis follows the same numerical methodology, where the droplets are considered to be sub-grid point sources. This approach is consistent with the pioneering experimental flame-droplet analysis by Burgoyne and Cohen (1954), in which the largest droplet size did not exceed approximately 10% of the unstrained laminar flame thickness of the stoichiometric mixture, $\delta_{th} = (T_{ad} - T_0)/\max(|\nabla T|)_L$, where T_{ad} is the adiabatic flame temperature, T_0 is the unburnt gas temperature and subscript L denotes unstrained laminar premixed flame for a stoichiometric fuel-air mixture. Since one typically needs more than 10 grid points in order to resolve the unstrained laminar flame thickness, the assumption of sub-grid point source is expected to be valid for the range of droplet sizes encountered for typical premixed flame-droplet interaction.

The objective of this paper is to present both the similarities between premixed flame propagation and droplet-laden flame propagation exhibited by smaller droplets and to highlight the differences observed in the case of larger droplets. The mathematical and numerical implementation pertaining to the 3D DNS simulations conducted here will be presented in the next section (i.e. Section 2). Following this, results will be presented and subsequently discussed in Section 3. Finally the main findings of this paper will be summarised and conclusions will be drawn in the final section (i.e. Section 4).

2. Mathematical & Numerical Modelling

This study was performed using a well-known 3D DNS code SENGGA, where the governing equations of mass, momentum, energy and species conservation were solved in non-dimensional form. Interested readers are referred to Jenkins and Cant (1999) for more information regarding the numerical schemes and bench-marking of this code. The simulations were performed in a canonical configuration within a rectangular domain of dimensions $30\delta_{th} \times 10\delta_{th} \times 10\delta_{th}$. The density, temperature and mean velocity fields have been initialised based on an unstrained planar 1D laminar stoichiometric (i.e. gaseous equivalence ratio $\phi_g = 1.0$) premixed flame solution. For the purpose of the 3D simulations the gaseous fuel profile in the region $|\dot{\omega}_F|/\max(|\dot{\omega}_F|) \leq 0.01$ ($\dot{\omega}_F$ is the fuel reaction rate) was reduced to the saturated vapour density to allow for the introduction of liquid fuel whilst maintaining an overall equivalence ratio equal to that of the original gaseous equivalence ratio (i.e. $\phi_{ov} = \phi_d + \phi_g = 1.0$, where ϕ_d is the fractional equivalence ratio due to the fuel in droplet form). The planar flame solution was specified in such a manner that the direction of flame propagation aligns with negative x -direction and $|\dot{\omega}_F|/\max(|\dot{\omega}_F|) \leq 0.01$ extends up to $1/3$ of the way across the domain (i.e. at $x/\delta_{th} = 10.0$). Boundaries in the x -direction were treated as inlet (LHS) and outlet (RHS), and were subject to partially non-reflecting Navier Stokes Characteristic Boundary (NSCBC) conditions (Poinsot and Lele, (1992)). Transverse directions were treated as periodic. The droplets were mono-disperse and were initially distributed uniformly in the region $0.0 \leq x/\delta_{th} \leq 10.0$ and throughout the y - and z -directions. The fuel was considered to be n-decane, $C_{10}H_{22}$, for the current analysis, which, due to its low evaporation rate, enables easier analysis of flame-droplet interaction compared to more volatile fuels (e.g. n-heptane). The modified one-step Arrhenius-type chemical mechanism proposed by Tarrazo et al. (2006) was used for the sake of computational economy. This chemical mechanism includes equivalence ratio dependence of activation energy and heat of combustion, which enables the correct prediction of equivalence ratio dependence of unstrained laminar burning velocity in hydrocarbon-air flames especially

for fuel-rich mixtures.

The mathematical formulation follows that of Reveillon and Vervisch (2005). The generic gas phase transport equation can be given as:

$$\frac{\partial \rho \varphi}{\partial t} + \frac{\partial \rho u_j \varphi}{\partial x_j} = \frac{\partial}{\partial x_j} \left(\frac{\rho \nu}{\sigma_\varphi} \frac{\partial \varphi}{\partial x_j} \right) + \dot{\omega}_\varphi + \dot{S}_\varphi, \quad (1)$$

where $\varphi = \{1, u_j, e, Y_i\}$ for the conservation equations of mass, momentum, energy and mass fractions respectively, where u_j is the velocity in the j^{th} direction, e is the stagnation internal energy (i.e. $e = \int_{T_{ref}}^T C_v dT' + \frac{1}{2} u_k u_k$, where C_v is the specific heat at constant volume, and T and T_{ref} are instantaneous and reference temperatures respectively) and $Y_{i=F,O}$ is the mass fraction for the fuel and oxidiser respectively. The $\dot{\omega}_\varphi$ term corresponds to reaction rate and \dot{S}_φ is the source term due to droplet evaporation, which is linearly interpolated from the droplet's sub-grid position, \vec{x}_d , to the eight surrounding nodes. Other variables are ρ density, ν kinematic viscosity and σ_φ an appropriate Schmidt number corresponding to φ .

It is often useful to characterise the mixture inhomogeneity using the mixture fraction, Z , which is defined as (Wandel et al., 2009):

$$Z = \frac{Y_F - Y_O/s + Y_{O,\infty}/s}{Y_{F,\infty} + Y_{O,\infty}/s}, \quad (2)$$

where $Y_{F,\infty} = 1.0$ is the fuel mass fraction in the pure fuel stream, $Y_{O,\infty} = 0.2331$ is the oxygen mass fraction in the pure air stream and is the ratio of oxygen to fuel mass under stoichiometric condition, which for $C_{10}H_{22}$ -air combustion assumes a value of 3.49. Moreover, the state of chemical reaction can be characterised in terms of a reaction progress variable c , which increases monotonically from 0 in unburned gas to 1 in fully burned products. Here c is defined based on the oxidiser mass fraction Y_O as:

$$c = \frac{(1 - Z)Y_{O,\infty} - Y_O}{(1 - Z)Y_{O,\infty} - \max\left(0, \frac{Z_{st} - Z}{Z_{st}}\right) Y_{O,\infty}}, \quad (3)$$

where $Z_{st} = 0.0625$ is the stoichiometric mixture fraction. It is possible to derive the transport equation for c from the transport equations for Y_F , Y_O and Z , it is given by:

$$\rho \frac{\partial c}{\partial t} + \rho u_j \frac{\partial c}{\partial x_j} = \frac{\partial}{\partial x_j} \left(\rho D \frac{\partial c}{\partial x_j} \right) + \dot{\omega}_c + \dot{S}_c + \dot{A}_c, \quad (4)$$

where D is the molecular diffusivity and $\dot{\omega}_c$, \dot{S}_c and \dot{A}_c are the chemical reaction rate, droplet source and cross-scalar dissipation terms respectively. The definition of these terms varies depending on the local value of Z in accordance with the denominator of (i.e. depending on $Z > Z_{st}$ or $Z \leq Z_{st}$). Their definitions are summarised in Table 1 and are dependent on the oxidiser reaction rate, $\dot{\omega}_O$, and the droplet 'source' term contribution to the mixture fraction transport equation, $\dot{S}_Z = \frac{\dot{S}_F}{(Y_{F,\infty} + Y_{O,\infty}/s)}$, where \dot{S}_F is the droplet source term in the fuel mass fraction transport equation. In the present analysis the simulations for droplets of different diameters were carried out for a common group number, G , which was defined according to Chiu and Liu (1977) as:

$$G = 3 \left(1 + 0.276 \left(\frac{S_L a_d}{\nu} \right)^{1/2} Sc^{1/3} \right) Le N^{2/3} \frac{a_d}{s_d}, \quad (5)$$

where S_L , a_d , Sc , Le , N and s_d are the unstrained laminar flame speed for the stoichiometric mixture, droplet diameter, Schmidt number, Lewis number, droplet number in a volume $(10\delta_{th})^3$ (in which droplets were

Table 1. Z -dependent terms in c transport equation.

	$Z > Z_{st}$	$Z \leq Z_{st}$
\dot{W}_c	$\frac{-\dot{\omega}_O}{(1-Z)Y_{O,\infty}}$	$\frac{-Z_{st}\dot{\omega}_O}{(1-Z_{st})ZY_{O,\infty}}$
\dot{S}_c	$\frac{-Y_O\dot{S}_Z}{(1-Z)^2Y_{O,\infty}}$	$\frac{-Z_{st}(Y_{O,\infty}-Y_O)\dot{S}_Z}{(1-Z_{st})Z^2Y_{O,\infty}}$
\dot{A}_c	$\frac{-2\rho D}{(1-Z)}\frac{\partial c}{\partial x_j}\frac{\partial Z}{\partial x_j}$	$\frac{2\rho D}{Z}\frac{\partial c}{\partial x_j}\frac{\partial Z}{\partial x_j}$

distributed in the current simulations) and mean inter-droplet spacing respectively. A group number $G \ll 1.0$ indicates combustion of individually burning droplets, whereas $G \gg 1.0$ indicates external sheath combustion. The present study investigates droplet combustion belonging to the latter regime.

A detailed parametric analysis has been carried out in this paper based on a reference case where the liquid fuel is introduced in the form of droplets of diameter $a_{d,b} \approx 0.01\delta_{th}$ (subscript b denotes the base case) with the droplet number chosen in order to maintain the overall equivalence ratio $\phi_{ov} = 1.0$, based on the prescribed initial conditions. This gives rise to a group number $G \approx 572$. In order to carry out a parametric analysis with respect to the reference case, both N and a_d are altered to maintain $G \approx 572$. This gives rise to a much inflated overall equivalence ratio for the larger droplets. Table 2 gives a summary of these values. Each of the gaseous/droplet-laden cases were investigated under turbulent flow field conditions with the following values of normalised rms turbulent velocity fluctuation $u'/S_L = \{0.0, 4.0, 8.0\}$ and normalised longitudinal integral length scale $L_{11}/\delta_{th} = \{1.0, 1.8, 2.5\}$.

Table 2. Droplet diameters and overall equivalence ratios.

$a_d/a_{d,b}$	gaseous (premixed)	1.0	5.0	10.0
ϕ_{ov}	1.0	1.0	20.7	79.9

3. Results & Discussion

For the present analysis simulations have been carried out for a duration $t = 2.0t_{chem}$, where $t_{chem} = \delta_{th}/S_L$ is the chemical timescale, corresponding to at least 3 initial eddy turn-over times. This simulation remains either greater than or comparable to several analyses (e.g. Grout (2005), Han and Huh (2008)) which contributed significantly to the fundamental understanding of premixed turbulent combustion. For ease of reference the simulations are grouped in 7 categories, as shown in Table 3. The premixed case ($a_d/a_{d,b} = 0$) with the same turbulent characteristics as the corresponding droplet cases are grouped together for ease of comparison. The temporal evolution of the global rms velocity fluctuation normalised by its initial value, u'/u'_0 , and normalised volume-integrated burning rate, Ω_T/Ω_L (where $\Omega = \langle \int_V |\dot{\omega}_F| dV \rangle$ and subscript T denotes turbulent flow conditions), for group (2) are shown in Fig. 1. It is apparent that u'/u'_0 and Ω_T/Ω_L do not change rapidly with time when the statistics were extracted. The temporal evolution of Ω_T/Ω_L is comparable to premixed combustion for small droplets, once initial evaporation has taken place (see also Fig. 4), but its value decreases with increasing a_d . The instantaneous fuel mass fraction field in the central $x_1 - x_2$ plane at $t = 2.0t_{chem}$ for cases belonging to groups (1) (left panel) and (2) (right panel) (see Table 3) are shown in Fig. 2. It is evident from Fig. 2 that the flame structure in the smallest turbulent droplet case is comparable to that of the turbulent premixed case, whereas the flame structures of the two

Table. 3. Grouping of simulations.

group	flow type	$a_d/a_{d,b}$	u'/S_L	L_{11}/δ_{th}
(1)	laminar	0, 1, 5, 10	n/a	n/a
(2)	turbulent	0, 1, 5, 10	8.0	1.0
(3)	turbulent	0, 1, 5, 10	8.0	1.8
(4)	turbulent	0, 1, 5, 10	8.0	2.5
(5)	turbulent	0, 1, 5, 10	4.0	1.0
(6)	turbulent	0, 1, 5, 10	4.0	1.8
(7)	turbulent	0, 1, 5, 10	4.0	2.5

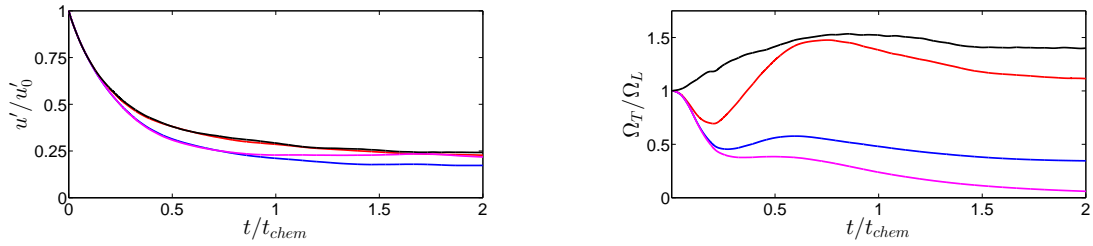


Fig. 1. Temporal evolution of normalised (left) velocity fluctuations and (right) burning rates for group (2). Premixed case (black) and droplet sizes $a_d/a_{d,b} = 1, 5, 10$ (red, blue and magenta respectively).

larger turbulent droplet cases are significantly different from the premixed case. Moreover, it can be seen in the turbulent cases that the smallest droplets barely enter the reaction zone with most having evaporated entirely before reaching the flame, whereas the larger droplets penetrate well into the reaction zone. In some large droplet cases the droplets continue to evaporate in the burned gas region with the gaseous fuel released then diffusing back towards the reaction front. On the other hand, all droplets in the laminar cases remain confined to the unburned gas region. Although the effect of the droplets is apparent from the wrinkled iso-surfaces, as visualised experimentally by Lawes and Saat (2011). Furthermore, the fuel mass fraction in the unburned gas for all droplet cases assumes much smaller values than the value obtained for the stoichiometric premixed flame. Thus, although $\phi_{ov} \gg 1.0$ for the two larger droplets, the gaseous equivalence ratio ϕ_g is much more modest due to the slow rate of evaporation of the liquid fuel. This can be substantiated from Fig. 3(a), which shows the probability density function (PDF) of the equivalence ratio in gaseous phase for the reaction progress variable c —range $0.01 \leq c \leq 0.99$ for all the droplet cases. The premixed flame case yields a δ -function located at $\phi_g = 1.0$ and thus is not shown here. The PDFs of ϕ_g show high probability of finding fuel-lean mixtures. The more significant peaks at higher values of equivalence ratio ϕ_g in the laminar cases (i.e. group (1)) can be attributed to the lack of turbulence-driven diffusion, which allows local pockets of fuel-rich gases to develop, whereas the effect of turbulent mixing is evident in all other groups (2-7). The noticeable fluctuations in PDF(ϕ_g) for the laminar group (1) are also due to the lack of turbulent mixing. It is notable that there is no significant difference between the two levels of turbulent velocity fluctuations which have been investigated in this analysis, indicating that either is sufficient to mix gaseous evaporated fuel.

It can be seen from Fig. 2 that fuel is consumed in a thin zone separating the unburned and burned gases in premixed flame, but the reaction zone becomes progressively thicker with increasing droplet size. The

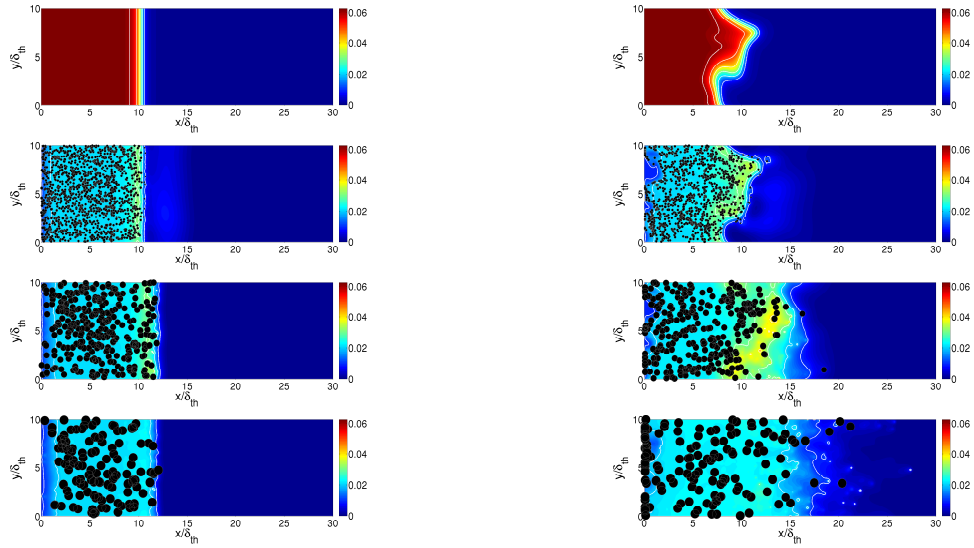


Fig. 2. Fuel mass fraction field at $t = 2.0t_{chem}$ for (top to bottom) premixed and small, medium and large droplets under (left panel) laminar and (right panel) turbulent flow conditions (laminar cases group (1) and turbulent cases group (2) in Table 3). White contour lines are the iso-surfaces $Y_F = \{0.01, 0.02, 0.03, 0.04, 0.05, 0.06\}$.

thickening of reaction zone in droplet cases can be confirmed from Fig. 3(b), which shows the normalised mean values of the magnitude of the gradient of (i.e. surface density function (SDF)= $|\nabla c|$) conditional on c values across the flame front. Dimensionally the inverse of the normalised SDF, $|\nabla c| \times \delta_{th}$, can be understood as a measure of the turbulent flame thickness relative to that of the unstrained laminar flame thickness (i.e. $|\nabla c| \sim 1/\delta$, where δ is the local flame thickness). All premixed cases (black lines) attain a peak value of $|\nabla c| \times \delta_{th} \approx 1.0$ in the region of $c = 0.6$, whereas the droplet cases fail to attain such a high value, instead showing a monotonic decrease in $\max(|\nabla c| \times \delta_{th})$ with increasing droplet diameter (red to blue to magenta). There is also an increase in the value of c at which $\max(|\nabla c| \times \delta_{th})$ is attained, and once again the increase appears to be greater for larger droplet diameter. Figure 3(a) shows high probability of finding fuel-lean mixtures in the reaction zone for large droplets and thus these cases show thicker flame due to small values of burning velocity in fuel-lean mixtures. This is consistent with the fuel mass fraction fields shown in Fig. 2, which shows that fuel consumption takes place over a thick region for large values of a_d , in contrast to a thin reaction zone for premixed and small droplet cases. This further indicates that the underlying combustion in large droplet cases takes place over a distributed region and possibly shows the attributes of the broken reaction zones regime (Peters, 2000).

The findings from Figs. 2-3 indicate that the presence of droplets is likely to significantly affect the internal reaction-diffusion balance of the flame. This can be demonstrated by examining the terms on the RHS of the reaction progress variable c transport equation (Eq. 4.). The mean variations of $\nabla \cdot (\rho D \nabla c)$, $\dot{\omega}_c$, \dot{A}_c and \dot{S}_c conditional on c across the flame front for the cases belonging to groups (1-2) are shown in Fig. 4, which reveal a number of important insights into the effects of droplets on the internal structure of the flame. These aspects apply to both turbulent and laminar cases and can be summarised as:

- The mean contribution of the term \dot{S}_c arising from the evaporation of droplets remains negligible in comparison to other terms for all droplet diameters. It is also negative (i.e. a sink term) in all droplet cases considered here.
- The mean behaviour of $\nabla \cdot (\rho D \nabla c)$ and $\dot{\omega}_c$ for smallest droplet (red) case follow closely the corresponding terms in the premixed flame case.

- The cross-scalar dissipation contribution, \dot{A}_c , plays a key role in the droplet cases and its mean contribution remains comparable to the mean values of $\nabla \cdot (\rho D \nabla c)$ and $\dot{\omega}_c$. The larger peak values attained by smaller droplets in the laminar case arise due to greater mixture inhomogeneities which develop under laminar flow conditions.
- The most significant difference is observed in the behaviour of the reaction rate term, $\dot{\omega}_c$. The mean contribution of this term for droplet combustion, although non-zero, is up to an order of magnitude smaller than the corresponding term in the premixed flame. It has been demonstrated in Fig. 3(a) that the probability of finding fuel-lean mixtures increases within the reaction zone for large droplet sizes, which gives rise to reduced reaction rate in large droplet cases compared to the reaction rate in stoichiometric premixed flame case. The reduced strength of $\dot{\omega}_c$ in comparison to $\nabla \cdot (\rho D \nabla c)$ for large a_d is again indicative of broken reaction zones regime combustion, where the effects of chemical reaction are weak and molecular diffusion plays the dominant role in deciding the reaction-diffusion balance in the interaction between premixed flame and droplets.
- In general, turbulent and laminar cases show similar trends, although the magnitude of the terms is generally greater in laminar cases than in the corresponding turbulent ones.

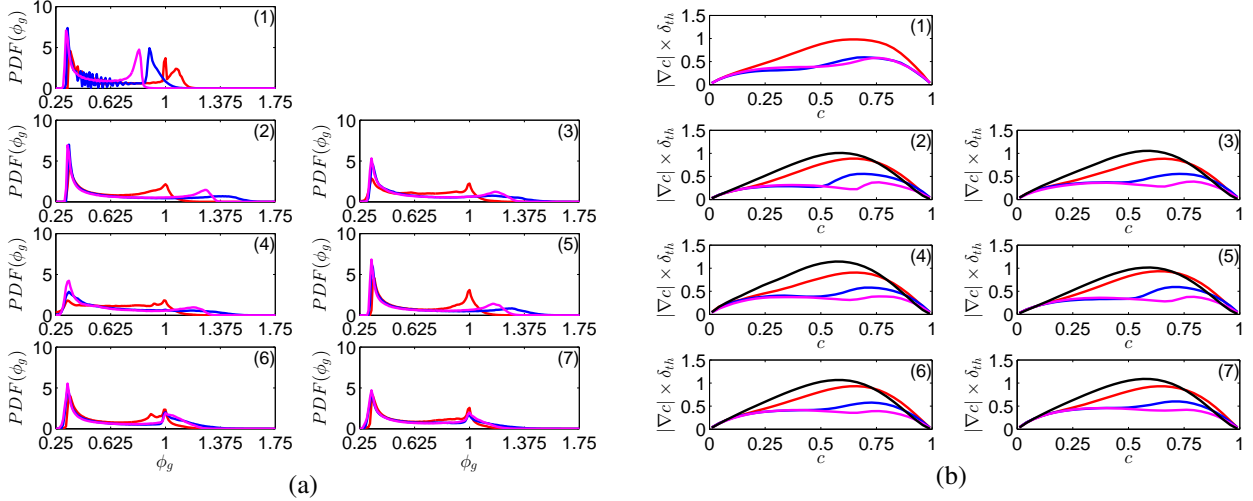


Fig. 3. (a) PDFs of ϕ_g for all droplet cases. (b) Variation of normalised SDF, $|\nabla c| \times \delta_{th}$, with c for all cases. Subplots are identified by group numbers shown in Table 3. Premixed cases are shown in black and droplet sizes $a_d/a_{d,b} = 1, 5, 10$ are shown in red, blue and magenta respectively.

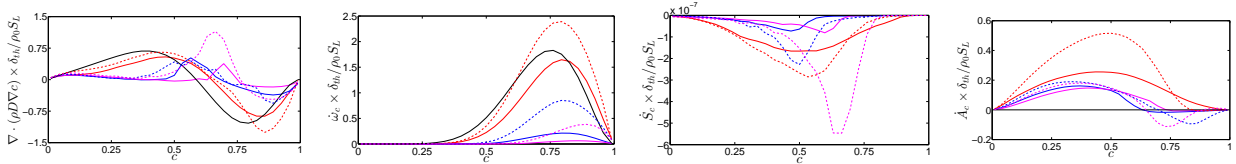


Fig. 4. Mean variation of terms in transport equation. Laminar cases (group (1), dashed lines) and turbulent cases (group (2), solid lines) are shown. The (turbulent) premixed case is shown in black and droplet sizes $a_d/a_{d,b} = 1, 5, 10$ are shown in red, blue and magenta respectively.

4. Conclusion

The interaction between premixed flame with droplets for n-decane-air has been analysed based on 3D DNS simulations for different values of overall equivalence ratio (ϕ_{ov}), rms velocity fluctuation (u'),

longitudinal integral length scale (L_{11}) and droplet diameter (a_d). It has been found that the turbulent flame structure remains qualitatively similar to the turbulent gaseous premixed flame for small droplet diameters, whereas the cases with large droplets exhibit significantly different features in comparison to the conventional premixed flame structure. Under turbulent conditions the large droplets penetrate the flame front and only evaporate entirely in the burned gas. In contrast, under laminar conditions no droplets penetrate the flame front, although there is evidence of droplet-induced wrinkling. The chemical reaction in droplet-laden flames takes place mostly in fuel-lean condition even for large values of overall equivalence ratio, as can be seen from the probability density function of equivalence ratio in gaseous phase ϕ_g in the droplet cases. The high probability of finding fuel-lean mixtures in the reaction zone gives rise to reduced reaction rate and thicker flame for large values of droplet diameter.

Acknowledgements

The authors would like to thank EPSRC for their financial support and N8 for use of the High Performance Computing facility.

References

- Aggarwal S. K. (1998). A review of spray ignition phenomena: Present status and future research. *Prog. Energy Combust. Sci.*, 24, 565-600.
- Bowen P. (2011). Combustion hazards posed by hybrid fuel systems “Proc. 5th Eur. Combust. Meeting”, Cardiff, UK.
- Burgoyne J. H. and Cohen L. (1954). The Effect of Drop Size on Flame Propagation in Liquid Aerosols. *Proc. Roy. Soc. Lond. A*, 225, 375-392.
- Chakraborty N., Mastorakos E. and Cant S. R. (2007). Effects of turbulence on spark ignition in inhomogeneous mixtures: a direct numerical simulation (DNS) study. *Combust. Sci. Technol.*, 179, 293-317.
- Chiu, H. H. and Liu, T. M. (1977). Group Combustion of Liquid Droplets. *Combust. Sci. Technol.*, 17, 127-142.
- Faeth G. M. (1987). Mixing, transport and combustion in sprays. *Prog. Energy Combust. Sci.*, 13, 193-345.
- Fernandez-Tarrazo E., Sanchez A. L., Linan A. and Williams F. A. (2006). A simple one-step chemistry model for partially premixed hydrocarbon combustion. *Combust. Flame*, 147, 32-38.
- Grout R.W. (2007). An Age-extended Progress Variable for Conditioning Reaction Rates. *Phys. Fluids*, 19, 105107.
- Han I. and Huh K.H. (2008). Roles of displacement speed on evolution of flame surface density for different turbulent intensities and Lewis numbers for turbulent premixed combustion. *Combust. Flame*, 152, 194-205.
- Jenkins K.W. and Cant R.S. (1999). DNS of turbulent flame kernels “Proc. 2nd AFOSR Conf. on DNS and LES”, Rutgers University, Kluwer Academic Publishers, pp. 192-202.
- Lawes M. and Saat A. (2011). Burning rates of turbulent iso-octane aerosol mixtures in spherical flame explosions. *Proc. Combust. Inst.*, 32, 2047-2054.
- Miller R. S. and Bellan J. (1999). Direct numerical simulation of a confined three-dimensional gas mixing layer with one evaporating hydrocarbon-droplet-laden stream. *J. Fluid Mech.*, 384, 293-338.
- Peters N. (2000). “Turbulent Combustion”, Cambridge Univ. Press, Cambridge, UK.
- Poinsot T. J. and Lele S.K. (1992). Boundary conditions for direct simulations of compressible viscous flows. *J. Comput. Phys.*, 101, 104-129.
- Reveillon J. and Vervisch L. J. (2005). Analysis of weakly turbulent dilute-spray flames and spray combustion regimes. *Fluid Mech.*, 537, 317-347.

Wandel A. P., Chakraborty N. and Mastorakos E. (2009). Direct numerical simulations of turbulent flame expansion in fine sprays. *Proc. Combust. Inst.*, 32, 2283-2290.